ELSEVIER

# Microstructures and electrical conductivity of nanocrystalline ceria-based thin films

Jennifer L.M. Rupp *, Ludwig J. Gauckler

*Institute of Nonmetallic Inorganic Materials, Department of Materials, Swiss Federal Institute of Technology, ETH Zurich,*
*Wolfgang-Pauli-Str.10, CH-8093 Zurich, Switzerland*

## Abstract

Ceria-based thin films are potential materials for use as gas-sensing layers and electrolytes in micro-solid oxide fuel cells. Since the average grain sizes of these films are on the nanocrystalline scale (<150 nm), it is of fundamental interest whether the electrical conductivity might differ from microcrystalline ceria-based ceramics. In this study, $CeO_2$ and $Ce_{0.8}Gd_{0.2}O_{1.9-x}$ thin films have been fabrication by spray pyrolysis and pulsed laser deposition, and the influence of the ambient average grain size on the total DC conductivity is investigated. Dense and crack-free $CeO_2$ and $Ce_{0.8}Gd_{0.2}O_{1.9-x}$ thin films were produced that withstand annealing up to temperatures of 1100 °C. The dopant concentration and annealing temperature affect highly the grain growth kinetics of ceria-based thin films. Large concentrations of dopant exert Zener drag on grain growth and result in retarded grain growth. An increased total DC conductivity and decreased activation energy was observed when the average grain size of a $CeO_2$ or $Ce_{0.8}Gd_{0.2}O_{1.9-x}$ thin film was decreased.
© 2006 Published by Elsevier B.V.

## 1. Introduction

Ceria-based thin films have attracted great interest as gas sensors [1] and electrolyte materials for solid oxide fuel cells operating at intermediate temperatures [2,3]. The major advantage of thin film $CeO_2$ gas sensor materials is the possibility to produce tiny semiconductor gas sensors [4–6] with quick response times in contrast to conventional sensors [7]. Operating micro-solid oxide fuel cells (μ-SOFCs) with gadolinia doped ceria (CGO) thin films as electrolytes is advantageous due to: (i) the high ionic conductivity at intermediate operating temperatures compared to state-of-the-art yttria-stabilized zirconia (YSZ) [3,8,9]; (ii) the possibility to combine low-cost ceramic thin film methods, such as spray pyrolysis, with traditional silicon micromachining technologies; and (iii) the reduction of the ohmic losses through the cell resulting in higher power outputs [10]. Due to these reasons, it is interesting to investigate the electrical properties of ceria-based thin films also for μ-SOFC applications.

Spray pyrolysis offers the possibility to produce dense ceramic films in an amorphous state. These films can be crystallized by heat treatment to nanocrystalline materials without columnar structures. It is known that nanocrystalline ceramics (with grains <150 nm) are characterized by a large amount of grain boundaries relative to the grain volume, resulting in changed oxygen stoichiometries, electrical properties and different reaction kinetics in comparison to microcrystalline ceramics [11–13]. In the 1980s, Christie and van Berkel examined the relationship of microstructure and electrical conductivity of sintered CGO pellets [14] and Wang and Nowick those of $CeO_2$ [15]. For CGO and $CeO_2$, the authors observed suppressed grain boundary conductivity while decreasing the grain size from several micrometers to roughly 1 μm and an enhanced conductivity for grains smaller than 1 μm. The lower conductivity for smaller grain sizes still larger than 1 μm was referred to in the literature as the "grain boundary effect". It was ascribed to resistive blocking layers of Si- or Ca-rich phases at grain boundaries [16,17]. Experimental results on nanocrystalline $CeO_2$ with grains <150 nm showed high electronic conductivity to be predominant, attributed to a partially reduced ceria [18–22]. Tschope and Birringer and Kim

* Corresponding author. Tel.: +41 43 632 56 51.
 *E-mail address:* jennifer.rupp@mat.ethz.ch (J.L.M. Rupp).

and Maier concluded that this observation cannot only be explained by the reduction of the segregated impurities per grain boundary in nanocrystalline materials [23,24]. The authors ascribed the high oxygen deficiency of nanocrystalline ceria to the small grain size and the enhanced grain boundary conductivity to the accumulation of $Ce^{3+}$ in the proximity of the grain boundary, giving rise to space charge distributions. Grain-size-dependent space charge modeling for $CeO_2$ predicts the following [25]: (i) transition from ionic to electronic conductivity with decreasing grain size in air; (ii) enhanced electronic conductivity of nanocrystalline compared to microcrystalline specimens; and (iii) change of activation energies, due to the temperature dependence of the space charge effect. In the case of nanocrystalline CGO, little electrical conductivity data as a function of sub-micron-grain size exist. Suzuki et al. reported that CGO films prepared by spin coating (grains 10–150 nm) show increased total conductivities and decreased activation energies when the grain size decreases [37]. However, it remains doubtful whether those experimental results can be attributed to the impact of space charges on electrical properties. In general, the extension of space charge regions is given by the Debye length (for details, see [26]) and is inversely proportional to the ionic strength—in this case, the gadolinia dopant concentration times the second power of the charge ($Gd'_{Ce}$) in the ceria lattice. Therefore, the extension of space charge regions in CGO should be reduced by some atomic layers (as the Debye length is shortened) and less impact on electrical properties should be observed. Recently, Tschope et al. investigated the impact of space charges on the overall electrical conductivity of microcrystalline ceria samples with different trivalent dopants [27]. For the dopants $La^{3+}$, $Gd^{3+}$ or $Y^{3+}$ in concentrations larger than approximately 5 at.% in microcrystalline $CeO_2$ samples, the space charge had no impact on the electrical properties. Kim and Maier quantitatively calculated the impact of space charges on the electrical properties of nanocrystalline $Ce_{0.85}Gd_{0.15}O_{1.9-x}$ sintered pellets with ~ 30 nm grain size. They confirmed a good agreement of the model with experimental results [24].

Less data exist that demonstrate the influence of grain size on the electrical conductivity in the nanometer grain size range, especially for thin films. In the present study the relation between electrical property and microstructure of nanocrystalline $CeO_2$ and CGO thin films is investigated and compared to data of bulk materials.

## 2. Experimental procedures

$CeO_2$ and CGO thin films were prepared by an airblast spray pyrolysis technique. In spray pyrolysis, a precursor solution is atomized to droplets that undergo pyrolytic decomposition upon hitting a heated substrate. Thereby, amorphous metal oxide films form, which can be crystallized by annealing to nano-crystalline microstructures. The process is described in detail elsewhere [28]. The CGO spray pyrolysis precursor solutions were made of 0.02 mol/l gadolinium chloride (Alfa Aesar, 99.9% purity) and 0.08 mol/l cerium nitrate (Alfa Aesar, 99% purity) dissolved in 33:33:33 vol.% ethanol, diethylene glycol monobutyl ether and 1-methoxy-2-propanol (all solvents from

Fluka Chemie, >99% purity). The same solvents and the cerium nitrate salt were used for the 0.1 mol/l $CeO_2$ precursor. Precursor solutions were fed to a spray gun (Compact 2000 KM, Bölhoff Verfahrenstechnik, Germany) with a liquid flow rate of 34.4 ml/h and atomized with 1.5 bar air pressure. The droplets produced in this manner were sprayed on a heated sapphire single crystal substrate (Stettler, Switzerland) at $310\pm10$ °C for 5 h. The working distance between the spray nozzle and the hot plate was 45 cm. Pulsed laser deposited (PLD) (Surface, Germany) CGO films were produced on sapphire substrates using a KrF excimer laser (248 nm wavelength). The PLD process was performed at 300 °C, at a pressure of $10^{-3}$ mtorr, with 10 Hz laser pulsed frequency, 200 mJ energy per pulse and at 60 mm target–substrate distance. PLD targets were produced by uniaxially and isostatically pressing (850 kN for 3 min) $Ce_{0.8}Gd_{0.2}O_{1.9-x}$ powders (Praxair, purity 99.9%). The pellets were heated up to 1400 °C at 3 °C/min, held at this temperature for 4 h and cooled at 5 °C/min to room temperature. The density of the pellets was evaluated using the Archimedes method and reached >98% of the theoretical value.

The electrical properties were measured using in-plane four-point measurements as shown in Fig. 1. For these, thin films were deposited through a shadow mask on the substrate, resulting in films of approximately 14 mm × 28 mm × 300–400 nm (length × width × film thickness). By a second shadow mask, four Pt electrodes of roughly 150 nm thickness were sputtered (SCD 050 Sputter Coater, Bal-Tec). On each sputtered Pt strip, a platinum wire was fixed with platinum paste (C 3605 P, Heraeus GmbH) to the substrate by two bonds of ceramic two component binder. The samples were then heated to the desired crystallization temperature, being either 800 °C, 900 °C, 1000 °C or 1100 °C, where the temperature was held for 10 h and cooled to 20 °C (3 °C/min). In a previous grain growth study on CGO spray pyrolyzed and PLD thin films, we reported that stable microstructures are established within the first 10 h of iso-thermal dwell, which is advantageous for this microstructure-conductivity study, as no time-activated grain growth has to be considered if the prior dwell temperature is not exceeded during the conductivity experiments [29]. Electrical measurements were preformed using a digital multimeter by DC four-point conductivity measurements (197 A, Keithley). The DC four-point conductivity experiments were performed at a given single voltage of maximal 4 V across the thin film as a function of temperature in air with 3 °C/min cooling and heating rates. Thin film microstructures were characterized using scanning electron
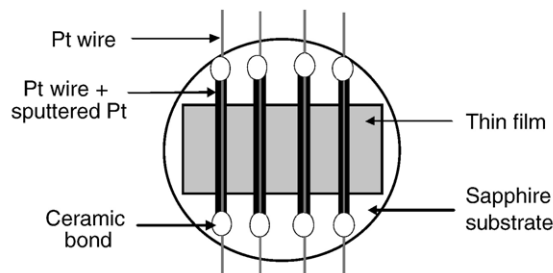


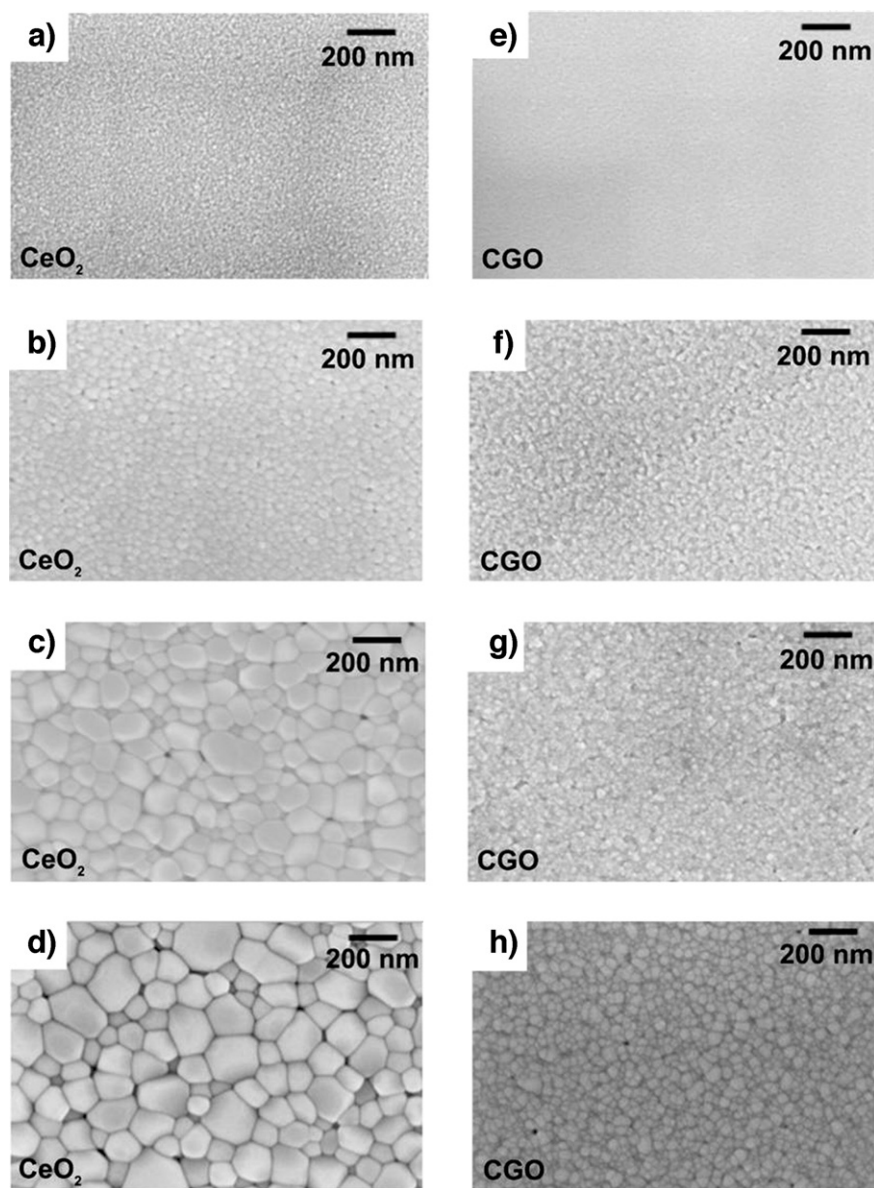Fig. 1. Sketch of thin film sample for four-point conductivity experiment.

Fig. 2. SEM microstructures of CeO$_2$ spray pyrolysis thin films annealed for 10 h at (a) 800 °C, (b) 900 °C, (c) 1000 °C and (d) 1100 °C, and of CGO spray pyrolysis thin films annealed for 10 h at (e) 800 °C, (f) 900 °C, (g) 1000 °C and (h) 1100 °C.

microscopy (SEM, Leo 1530, Germany). The average grain size was estimated from X-ray diffraction (XRD, Bruker AXS D8 Advance) data by means of the Scherrer equation for thin films with average grain sizes smaller than 80 nm [30]. Larger average grain sizes were characterized by measuring at least 300 grains in the SEM micrographs using the method of linear intercept with a grain intersection to grain size conversion factor of 1.56. For the average grain size evaluation, the program Lince 2.31 was used. Chemical composition was determined by energy dispersive X-ray spectroscopy (EDX, Leo 1530, Germany).

## 3. Results and discussion

### 3.1. Microstructure

The SEM plane views of CeO$_2$ (Fig. 2a–d) and CGO (Fig. 2e–h) spray pyrolyzed thin films are displayed in Fig. 2 as

a function of annealing temperature. Both CeO$_2$ as well as the CGO spray pyrolysis thin films exhibit dense and crack-free microstructures with no abnormal grain growth. As expected from solute drag theory [31], grain growth of the CeO$_2$ proceeds faster than the grain growth of the CGO thin films. For a moving grain boundary, the gadolinia distribution in the ceria

Table 1
Average grain sizes present after 10 h isothermal annealing at different temperatures for CeO$_2$ and CGO thin films

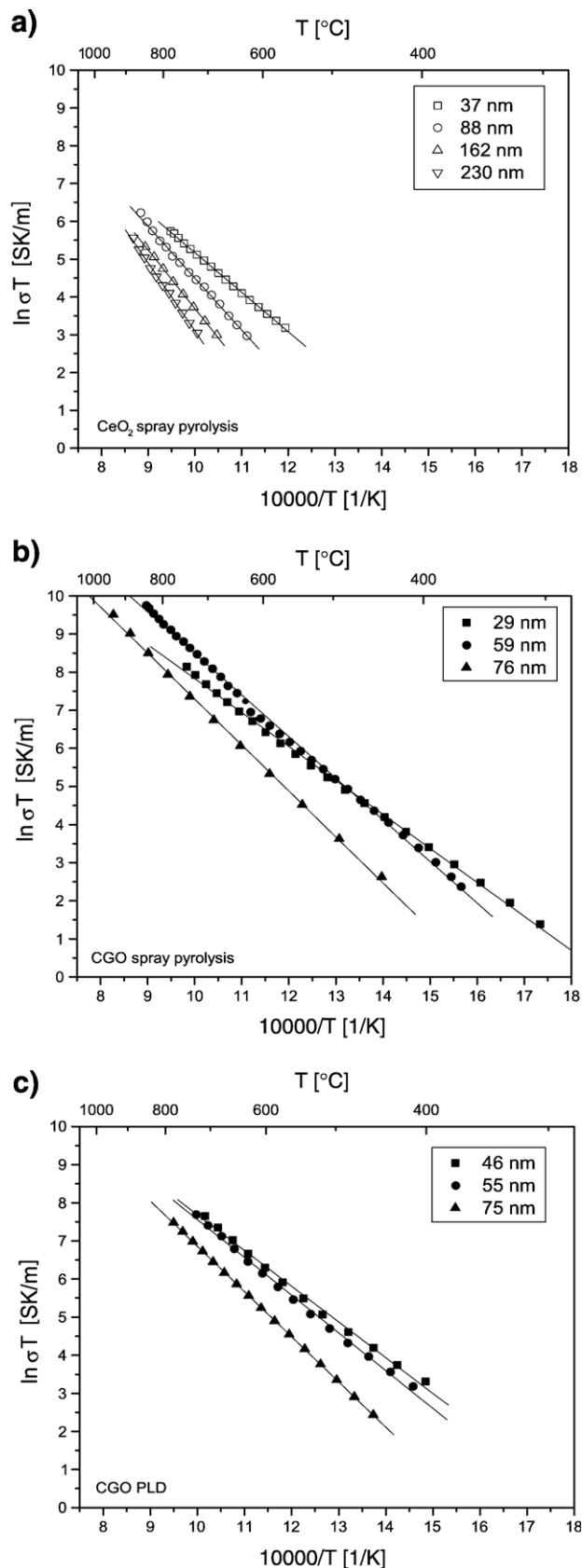| $T_{10 h}$ (°C) | Average grain size of CeO$_2$ spray pyrolysis (nm) | Average grain size of CGO spray pyrolysis (nm) | Average grain size of CGO PLD (nm) |
|---|---|---|---|
| 800 | 37 | 29 | 46 |
| 900 | 88 | 59 | 55 |
| 1000 | 162 | 76 | 75 |
| 1100 | 230 | 137 | – |

Fig. 3. Electrical conductivity for: (a) CeO$_2$ spray pyrolysis, (b) CGO spray pyrolysis and (c) CGO PLD thin films.

host lattice becomes asymmetric and acts as a drag force on grain growth. In CeO$_2$ films annealed at higher temperatures, it can be noticed that flat grain faces develop and small pores are created at grain triple junctions. This observation can be attributed to a grain size fraction exceeding in size that of the film thickness and was theoretically described earlier by Miller et al. [32]. The PLD-CGO thin film microstructures were dense and crack-free after annealing. Table 1 summarizes the determined average grain sizes of the CeO$_2$ and CGO spray pyrolysis and PLD thin films as a function of dwell temperature. The chemical composition of the films was analyzed by EDX using the cerium and gadolinium L-lines for the quantitative analysis. The analysis of the CGO spray pyrolysis and PLD films revealed 22±2 at.% (spray pyrolysis) and 25±1 at.% (PLD) of gadolinia in the ceria lattice. In the case of CeO$_2$ thin films, 100±1 at.% of ceria was detected. No additional elements could be detected by EDX in these thin films.

## 3.2. Electrical properties

The DC total conductivity ($\sigma$) of CeO$_2$ and CGO thin films was determined with respect to their different average grain sizes established after annealing at 800 °C, 900 °C, 1000 °C or 1100 °C. The activation energy $E_a$ of total conductivity was determined from the slope in the $\ln(\sigma T)$ vs. $1/T$ Arrhenius plot. In Fig. 3, the total electrical conductivity of (a) spray pyrolyzed CeO$_2$, (b) spray pyrolyzed CGO and (c) PLD CGO thin films as a function of temperature and average grain size are shown. The determined activation energies from these Arrhenius plots are summarized in Fig. 4 for all materials investigated with respect to average grain size. It is observed for the CeO$_2$ spray pyrolysis thin films that the total conductivity increases (Fig. 3a) and activation energy is lowered (Fig. 4) as the grain size decreases. The CeO$_2$ thin film with 37 nm average grain size exhibits 0.044 S/m at 600 °C, which is comparable to the conductivity of 0.05 S/m obtained by Chiang et al. [21] for sintered pellets of 10 nm average grain size. At this temperature, Suzuki et al. measured a lower conductivity of 0.01 S/m for spin-coated films
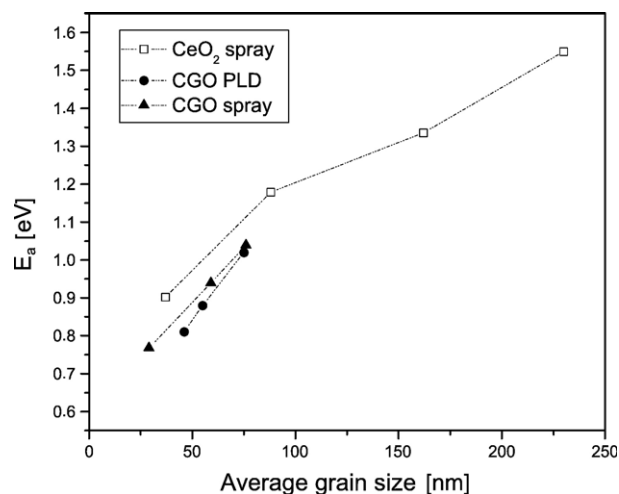


Fig. 4. Activation energy $E_a$ of electric conductivity for CeO$_2$ and CGO spray pyrolysis films and CGO PLD films as a function of average grain size.

of 30 nm average grain size [19]. Although the increase of the spray pyrolysis average grain size from 37 to 162 nm leads to a decrease of the total conductivity from 0.13 to 0.026 S/m at 700 °C, all measured conductivities are still by a factor of 2 to 10 higher than those determined for microcrystalline $CeO_2$ at 700 °C [33,34]. In Fig. 5a, the activation energies as a function of average grain size of $CeO_2$ prepared by spray pyrolysis are compared with the literature. Note that, beside thin films, results from sintered pellets (nano- and microcrystalline) are chosen also for comparison and used to check for possible preparation-related changes in activation energy, i.e. impurities or density. The literature comparison shows a strong activation energy decrease of 1.79 eV while reducing the average grain size from 5 μm to 26 nm. Moreover, decreased activation energies are observed once the grain size is decreased from the micro- to the nanocrystalline scale independently of the chosen preparation method.
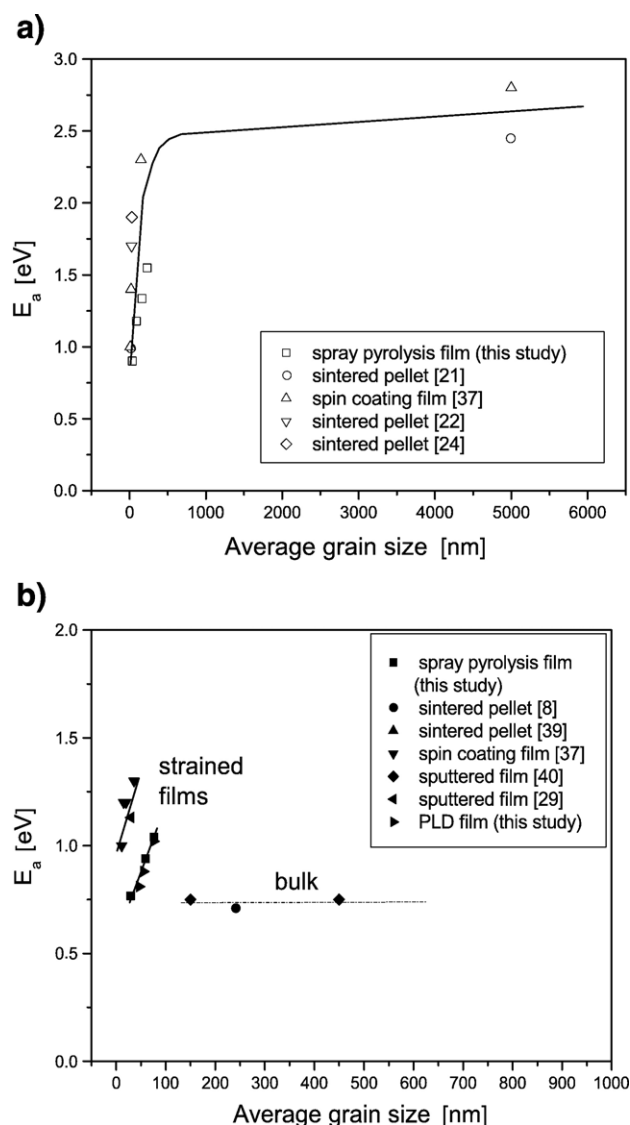


The decrease of total DC conductivity with decreasing average grain size for spray pyrolyzed $CeO_2$ thin films measured here agree with previous results for differently prepared bulk and thin film ceria samples (Fig. 5a) and are in accordance with the theoretical predictions of space charges affecting the electrical properties of nanocrystalline $CeO_2$ derived by Tschope et al. [25,33] and Maier [35,36].

DC total conductivities with respect to the average grain size of CGO spray pyrolyzed thin films are shown in Fig. 3b. The activation energies are summarized in Fig. 4. The lowest conductivity is present for samples with 76 nm average grain size. Fine-grained CGO films show higher conductivities (Fig. 3b). The activation energy decreases linearly from 1.04 to 0.77 eV with decreasing average grain size from 76 to 29 nm (Fig. 4). The comparison between the electrical properties of CGO spray pyrolyzed thin films and CGO spin-coated thin films [37] reveals the following characteristics: (i) Independent of thin film preparation method, the activation energy decreases with decreasing grain size. (ii) The total conductivities of all the spray pyrolyzed CGO thin films measured in this work are one order of magnitude higher than those of the spin-coated films. Total DC conductivities of 1.03 up to 3.83 S/m were measured for spray pyrolyzed thin films and 0.039 to 0.32 S/m for the spin-coated films at 700 °C.

Our previous study on CGO spray pyrolyzed thin films showed that a small concentration of carbon–below the detection limit of EDX and X-ray photoelectron spectroscopy–remains in the thin films even after annealing at 1000 °C [29,38]. Since the different average grain sizes of the spray pyrolysis samples were established by different annealing temperatures, different C concentrations might be present in the films depending on the present average grain size. The C concentration decreases with increasing grain size and annealing temperature. To elucidate whether different remaining C concentrations affect the conductivity, we conducted further grain-size-dependent conductivity measurements on CGO PLD thin films, for which no C containing precursors were involved in the film production. The Arrhenius plots of CGO PLD thin films are shown in Fig. 3c. The activation energies are summarized in Fig. 4. For the CGO PLD thin films, a similar decrease of activation energy and total DC conductivity with decreasing grain sizes was observed. The determined conductivity of CGO PLD thin films is close to those of the sprayed films, but again one order of magnitude higher than the one of the spin-coated films [37]. The total conductivity of the spray pyrolyzed and PLD thin films show a dependence on the average grain size. The spray pyrolysis and PLD thin films with grains smaller ~ 60 nm are in the conductivity range of microcrystalline samples (2.8–4.8 S/m at 700 °C, see literature review in Ref. [8] for details). For operation of these CGO films as electrolytes in fuel cells, further studies are still required to elucidate whether the here measured total conductivities are primary ionic or electronic in air.

In Fig. 5b, a literature overview on activation energies from differently prepared CGO samples as a function of average grain size is given. It is found that for pure CGO bulk samples with grains larger than 200 nm the activation energy remains

Fig. 5. Comparison of the activation energies $E_a$ of total conductivity for (a) $CeO_2$ and (b) $Ce_{0.8}Gd_{0.2}O_{1.9−x}$ as a function of average grain size.

almost constant at 0.71 eV [8,39,40]. In contrast, all CGO thin films show a decrease of activation energy with decreasing grain size, independent on the preparation method. In comparison with literature, the activation energies of the spin-coated films [37] are roughly 0.3 eV higher than those determined for spray pyrolysis or PLD films. We cannot observe one trend for the conductivity data of the thin films and the sintered pellets as a function of grain size. Although all CGO thin films show (i) higher activation energies than the sintered samples and (ii) decreased activation energy of total conductivity with decreasing grain size.

## 4. Summary and conclusions

Dense and crack-free thin films of $CeO_2$ and CGO were prepared by spray pyrolysis and pulsed laser deposition techniques.

Dopant concentration and annealing temperature affect the grain growth kinetics. Large concentrations of dopants exerted solute drag on grain growth and resulted in retarded grain growth of ceria-based thin films.

Grain-size-dependent electrical DC conductivity studies on the nanocrystalline scale (grains <150 nm) show that the activation energy of the total conductivity of $CeO_2$ decreases from 2.5 eV for microcrystalline to 0.9 eV in nano-scaled material (37 nm average grain size). From the present findings, it can be concluded that the conductivity and microstructure dependence of $CeO_2$ ceramics is in agreement with the currently discussed impact of space charge on defect distributions of nanocrystalline microstructures.

A strong decrease of activation energy and increase of total DC conductivity with decreasing grain size is reported for CGO thin films which differ substantially from microcrystalline CGO. Spray pyrolyzed and pulsed laser deposited CGO thin films with average grain sizes <60 nm show conductivities comparable to those measured in microcrystalline CGO. However, for operation of CGO films as electrolytes in fuel cells, further studies are required to proof whether the here measured total conductivities are primary ionic or electronic.

## Acknowledgement

## References

[1] P.T. Moseley, Sensors and Actuators. B, Chemical 6 (1992) 149.
[2] I. Taniguchi, R.C. van Landschoot, J. Schoonman, Solid State Ionics 160 (2003) 271.
[3] M. Mogensen, N.M. Sammes, G.A. Tompsett, Solid State Ionics 129 (2000) 63.
[4] I. Kosacki, H.U. Anderson, Sensors and Actuators. B, Chemical 48 (1998) 263.
[5] P. Jasinski, T. Suzuki, H.U. Anderson, Sensors and Actuators. B, Chemical 95 (2003) 73.
[6] H.-J. Beie, A. Gnorich, Sensors and Actuators. B, Chemical 4 (1991) 393.
[7] G. Sberveglieri, Sensors and Actuators. B, Chemical 23 (1995) 103.
[8] C. Kleinlogel, L.J. Gauckler, Solid State Ionics 135 (2000) 567.
[9] M. Gödickemeier, K. Sasaki, L.J. Gauckler, Journal of Electrochemical Society 144 (1997) 1635.
[10] D. Perednis, L.J. Gauckler, Solid State Ionics 166 (2004) 229.
[11] H.L. Tuller, Solid State Ionics 131 (2000) 143.
[12] I. Kosacki, T. Suzuki, H.U. Anderson, P. Colomban, Solid State Ionics 149 (2002) 99.
[13] J. Maier, Journal of the European Ceramic Society 24 (2004) 1251.
[14] G.M. Christie, F.P.F. van Berkel, Solid State Ionics 83 (1996) 17.
[15] D.Y. Wang, A.S. Nowick, Journal of Solid State Chemistry 35 (1980) 325.
[16] M. Gödickermeier, B. Michel, A. Orliukas, P. Bohac, K. Sasaki, L. Gauckler, Journal of Materials Research 9 (5) (1994) 1228.
[17] K. El Adham, A. Hammou, Solid State Ionics 9–10 (1983) 905.
[18] C.S. Chen, M.M.R. Boutz, B.A. Boukamp, A.J.A. Winnubst, K.J. de Vries, A.J. Burggraaf, Materials Science & Engineering. A, Structural Materials: Properties, Microstructure and Processing 168 (1993) 231.
[19] T. Suzuki, I. Kosacki, H.U. Anderson, P. Colomban, Journal of the American Ceramic Society 84 (2001) 2007.
[20] Y.M. Chiang, E.B. Lavik, I. Kosacki, H.L. Tuller, J.Y. Ying, Applied Physics Letters 69 (1996) 185.
[21] J.-M. Chiang, E.B. Lavik, I. Kosacki, H.L. Tuller, Journal of Electroceramics 1 (1) (1997) 7.
[22] A. Tschope, E. Sommer, R. Birringer, Solid State Ionics 139 (2001) 255.
[23] A. Tschope, R. Birringer, Journal of Electroceramics 7 (2001) 169.
[24] S. Kim, J. Maier, Journal of the European Ceramic Society 24 (2004) 1919.
[25] A. Tschope, Solid State Ionics 139 (2001) 267.
[26] I. Lubomirsky, J. Fleig, J. Maier, Journal of Applied Physics 92 (2002) 6819.
[27] A. Tschope, S. Kilassonia, R. Birringer, Solid State Ionics 173 (2004) 57.
[28] D. Perednis, O. Wilhelm, S.E. Pratsinis, L.J. Gauckler, Thin Solid Films 474 (2005) 84.
[29] J.L.M. Rupp, A. Infortuna, L.J. Gauckler, Acta Materialia 54 (2006) 1721.
[30] P. Scherrer, Nachrichten von der Königlichen Gesellschaft der Wissenschaft zu Göttingen: Mathematisch-physikalische Klasse 1 (1918) 98.
[31] J.W. Cahn, Acta Metallurgica 10 (1962) 798.
[32] K.T. Miller, F.F. Lange, D.B. Marshall, Journal of Materials Research 5 (1990) 151.
[33] A. Tschope, E. Sommer, R. Birringer, Solid State Ionics 139 (2001) 255.
[34] K. Eguchi, T. Setoguchi, T. Inoue, H. Arai, Solid State Ionics 52 (1992) 165.
[35] J. Maier, Solid State Ionics 157 (2003) 327.
[36] J. Maier, Zeitschrift für physikalische Chemie 217 (2003) 415.
[37] T. Suzuki, I. Kosacki, H.U. Anderson, Solid State Ionics 151 (2002) 111.
[38] J.L.M. Rupp, C. Solenthaler, P. Gasser, U.P. Muecke, L.J. Gauckler, Crystallization of amorphous ceria solid solutions, Acta Materialia, submitted for publication.
[39] D. Schneider, M. Godickemeier, L.J. Gauckler, Journal of Electroceramics 1 (1997) 165.
[40] X.-D. Zhou, W. Huebner, I. Kosacki, H.U. Anderson, Journal of the American Ceramic Society 85 (2002) 1757.